Journal of Catalysis 281 (2011) 188–197

Contents lists available at ScienceDirect

Journal of Catalysis

journal homepage: www.elsevier.com/locate/jcat

Controlled spillover in a single catalyst pellet: Rate modification, mechanism and relationship with electrochemical promotion

Danai Poulidi *, Maria Elena Rivas, Ian S. Metcalfe

School of Chemical Engineering and Advanced Materials, Newcastle University, Merz Court, NE1 7RU Newcastle-upon-Tyne, UK

ARTICLE INFO

Article history:
Received 16 January 2011
Revised 20 April 2011
Accepted 24 April 2011
Available online 25 May 2011

Keywords:
Metal–support interactions
Spillover
Catalyst promoters
Electrochemical promotion

ABSTRACT

The effect of spillover processes on the activity of a catalyst system consisting of a mixed oxygen ion and electronic conducting support $La_{0.6}Sr_{0.4}Co_{0.2}Fe_{0.8}O_{3-\delta}$ and a metal catalyst (Pt) were investigated. Two types of model single-pellet catalysts were used employing Pt deposited on both sides of a dense LSCF disc pellet. One of these single pellets employed highly disperse, physically non-continuous Pt, in contrast to studies on electrochemical promotion, while the other used a low dispersion continuous film. Driving forces for promoter migration were controlled through the manipulation of the oxygen chemical potential difference across the membrane. Catalyst rate modification was observed in all cases. However, it was found that there is a complex relationship between the rate modification, the driving forces for spillover and the geometrical arrangement of the catalyst on the support (i.e. catalyst dispersion).

1. Introduction

The importance of metal–support interactions and in particular the idea of a catalyst support having the ability to remotely modify the function of a catalyst through spillover processes (i.e. the migration of species from the catalyst to the support and vice versa) has been widely recognised (e.g. [1–7]). However, it is difficult to monitor or even influence spillover processes and therefore difficult to directly study their impact on catalyst activity. In this work, we study how chemical potential differences within a single catalyst pellet can cause a modification of catalyst behaviour (in practice such potential differences could, e.g., be due to compositional variations within a reactor). These chemical potential differences are experimentally recreated using a pellet exposed simultaneously to two different gas phase atmospheres. We show that the driving forces within the pellet modify the behaviour of the catalyst.

Catalyst promoters enhance the activity and selectivity of a catalyst [8]. While most promoters are added during catalyst preparation, their *in situ* supply is also attractive as it could allow the reversible control of catalytic activity. One way of reversibly introducing promoters is by exploiting spillover processes [9,10]. In electrochemical promotion of catalysis (EPOC) studies, porous, continuous metal film catalysts supported on dense, ceramic, ion-conducting membranes are employed, operated under closed circuit conditions; these systems are very different to 'real' catalysts and therefore may struggle to offer practical solutions for the catalysis industry while also failing to serve as representative model systems.

In any catalyst system, spillover may occur if a chemical potential difference exists for the spillover species within the catalyst system. Such a chemical potential difference will, in general, not be present unless the spillover species is consumed through reaction or lost from the surface of the catalyst system through, e.g. volatilisation. A reverse spillover process (defined as the migration of species from the support to the catalyst) will occur if the catalyst is more active than the support for the consumption of the spillover species. In this manuscript, the term spillover refers generally to reverse or back-spillover.

In a 'real' catalyst system ('real' refers to a dispersed active phase deposited upon a lower activity support phase), spillover will occur due to chemical potential difference within the catalyst, created either by the different activity of the catalyst and the support for a given reaction or simply by compositional variations within the reactor or in the vicinity of the catalyst pellet. In a 'real' catalyst system, there is no way to control these chemical potential differences that result in spillover, and therefore, it is not possible to control and study spillover processes. In order to be able to do so, a model system must be used. In this work, we have selected platinum (Pt) supported on an $La_{0.6}Sr_{0.4}Co_{0.2}Fe_{0.8}O_{3-\alpha}$ (LSCF) pellet as the catalyst system. As a mixed oxygen ion and electron conductor (MIEC) [11,12], LSCF, is able to capture oxygen from the gas phase atmosphere through oxygen adsorption and subsequent electronation as shown in Fig. 1. The resulting oxygen ions (implicated as spillover-mediated promoters in EPOC studies e.g. [13,14]) can be supplied from the LSCF support to the surface of the platinum by either surface or bulk diffusion in the LSCF support followed by spillover onto the catalyst surface.

* Corresponding author.
E-mail address: danai.poulidi@ncl.ac.uk (D. Poulidi).

0021-9517/$ - see front matter © 2011 Elsevier Inc. All rights reserved.
doi:10.1016/j.jcat.2011.04.016

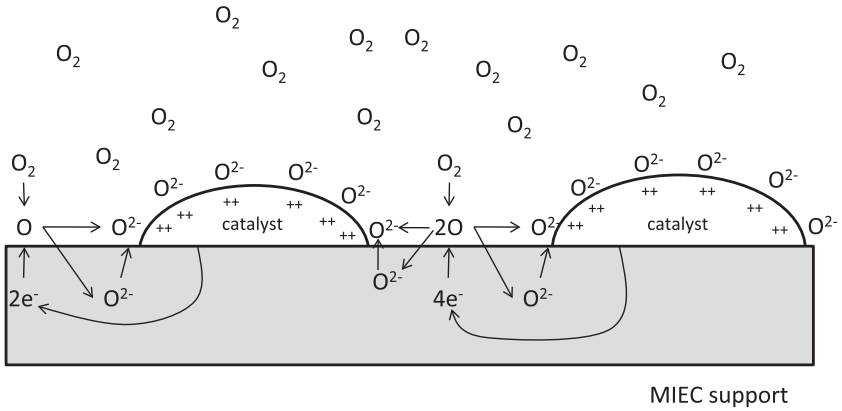

Fig. 1. Schematic representation of the oxygen spillover mechanisms on a mixed ionic and electronic conducting membrane.

We now form a pellet of LSCF with Pt catalysts of the same morphology on both sides. The pellet is dense, and there is no route for gas phase transport from one side of the pellet to the other. With both sides exposed to the same gas phase atmosphere, there would be no chemical potential difference across the membrane and hence no net flux of oxygen ions across the membrane (for the sake of clarity in the discussion, the chemical potential difference across the membrane refers to the difference between the catalyst–support gas phase interface (three-phase-boundary, *tpb*) on either side of the membrane). Both catalysts would exhibit the same catalytic activity, as shown in Fig. 2a. However, as shown in Fig. 2a, it remains possible to have oxygen spillover as a result of the oxygen captured directly from the gas phase due to surface chemical potential differences on either side of the membrane. These surface chemical potential differences (possibly between the LSCF support and the Pt catalyst), as previously mentioned, could be due to differences in catalytic activity between catalyst and support and would exist even in the absence of chemical potential differences across the membrane. Overall oxygen capture involves oxygen adsorption,

$$O_2 \leftrightarrow 2O_{ads} \tag{1}$$

oxygen capture itself, i.e., reaction with electrons from the mixed conducting support to form oxygen ions either in the bulk of the support or in/on the surface,

$$O_{ads} + 2e^-_{supp} \leftrightarrow O^{2-}_{supp} \tag{2}$$

$$O_{ads} + 2e^-_{supp} \leftrightarrow O^{2-}_{ads} \tag{3}$$

and migration of the ionic oxygen species by bulk or surface diffusion to the *tpb*,

$$O^{2-}_{supp} \leftrightarrow O^{2-}_{tpb} \tag{4}$$

$$O^{2-}_{ads} \leftrightarrow O^{2-}_{tpb} \tag{5}$$

The spillover of oxygen species captured directly from the same gas atmosphere that the Pt catalyst is exposed to will be referred to as local spillover in this manuscript.

If we modify the gas phase conditions on one side of the pellet, we create a driving force for oxygen ion transfer across the pellet that initiates the supply (or removal) of oxygen species to the catalyst due to the difference in the oxygen chemical potential difference across the membrane. The spillover of oxygen species supplied to the catalyst due to this oxygen chemical potential

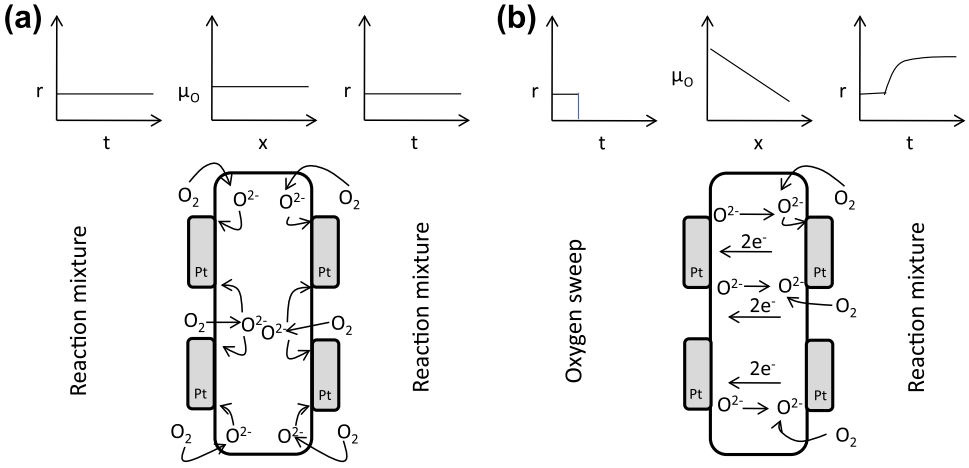

Fig. 2. Schematic representation of the catalyst modification on a dual chamber MIEC pellet supporting a metallic catalyst. (a) Symmetrical operation: under identical reaction conditions, no oxygen chemical potential difference should exist across the pellet (depicted as a constant chemical potential as a function of distance across the pellet) on the schematic. The oxygen spillover on either side of the pellet (supplied local spillover phenomena) should be the same, and the steady state reaction rates (presented as rate transients in the schematic) should be equal (electronic fluxes are not shown for clarity). (b) Operation under an oxygen chemical potential difference using an oxygen sweep: a driving force for the migration of oxygen across the pellet is created that increases the oxygen spillover from the bulk of the membrane (μO is depicted as a function of distance, *x*, across the membrane at a time when the new steady state has been reached – the gradient of μO with respect to *x* is shown as being constant for illustrative purposes but this would not necessarily be the case) and increases the reaction rate on the reaction side to a new steady state value, while the reaction rate on the sweep side disappears.

Table 1
Summary of catalysts used in this work and listing of relevant experiments and figures for each catalyst pellet.

	Support configuration	Catalyst morphology	Experiment	Results shown
Pellet A[a]	Disc membrane	Film	Kinetic measurements under $\Delta\mu O$, O_2 sweep	Fig. 4
Pellet B	Disc membrane	Film	Kinetic measurements under $\Delta\mu O$, O_2, H_2 sweeps	Fig. 5
Pellet C	Disc membrane	Film	Kinetic measurements under $\Delta\mu O$, O_2, H_2 sweeps	Fig. 6
Pellet D	Disc membrane	Film	Kinetic measurements under $\Delta\mu O$, O_2 sweep, oxygen titration	Fig. 7
Pellet E	Disc membrane	Film	Kinetic measurements under no $\Delta\mu O$, symmetrical operation, O_2 sweep	Fig. 8
Pellet F	Disc membrane	Film	Kinetic measurements under no $\Delta\mu O$, symmetrical operation, H_2 sweep	Fig. 8
Pellet G	Disc membrane	Dispersed	Kinetic measurements under $\Delta\mu O$, O_2 sweeps	Fig. 9

[a] Work conducted on Pellet A has already been published in [21].

difference across the membrane will be referred to as remote spillover. The terms local and remote spillover used in this manuscript refer to the origin of the driving force for spillover (surface oxygen chemical potential differences in the locality of the *tpb* on one side of the membrane versus imposed oxygen chemical potential difference across the membrane) and not the mechanism of promoter supply (i.e. bulk or surface diffusion). As a consequence of remote spillover occurring under an oxygen chemical potential difference across the membrane, a change in reaction rate on both sides of the pellet might be expected to occur. The rate change as a result of spillover should be clearly seen on the side of the pellet that has unchanged gas phase conditions, as shown in Fig. 2b.[1]

The role of what is referred to here as local spillover was acknowledged in the early work by Metcalfe and Sundaresan [15] where it was postulated that highly dispersed catalysts of Pt-TiO_2 outperformed Pt-YSZ of the same catalyst loading and dispersion due to the ability of the mixed conducting TiO_2 support to capture oxygen directly from the gas phase. In addition, in EPOC experiments conducted with a thin TiO_2 layer interlaid between the ionic conducting support (YSZ) and the Pt catalyst, it was found that due to the local spillover, the observed promotion of the Pt–TiO_2–YSZ catalyst was higher than what was obtained on a Pt–YSZ system [16]. The same effect was observed when working with Rh–TiO_2 catalysts for EPOC [17].

In our previous work, we have proved the feasibility of using such a membrane system in order to induce and monitor catalytic rate changes in a Pt catalyst supported on an LSCF membrane [18,19]. Here, we now extend this work to consider the processes that may be occurring within the whole of a single catalyst pellet and the role these processes have on pellet activity.

2. Experimental

The experiments discussed in this manuscript were performed using two different types of catalysts shown in Table 1; (a) a continuous, porous Pt film catalyst supported on LSCF disc membranes (film), (b) Pt dispersed on LSCF powder supported on LSCF disc membranes (dispersed). Due to high breakage rates of the LSCF disc membranes, several film catalyst pellets were used as shown in Table 1. This explains the difference between the reaction rates of the kinetic experiments discussed later. The reaction studied during the kinetic experiments was ethylene oxidation. The temperature of operation for the kinetic experiments was restricted between 400–450 °C in order to obtain the necessary oxygen flux to supply the promoter onto the catalyst and observe promotion (promotion is not seen at much higher temperatures [20]). All experiments were performed under atmospheric pressure, and all volumetric flow rates are given at STP.

[1] It is important to note that when using a MIEC pellet as a support, the catalyst can be in a non-continuous form. The processes illustrated in Fig. 2 will be conceptually the same for a continuous and a non-continuous support. This is a significant advantage of the MIEC supporting membranes as they could be used to support highly dispersed high surface area catalysts for applications that utilise and manipulate spillover processes for catalytic modification.

2.1. Catalyst characterisation

The preparation method of the film catalysts has been described in detail in our previous publications [19]. In brief, approximately 2.2 g of commercial LSCF powder (Praxair) was uniaxially pressed to 20-mm-diameter pallets at 4 tons; the pellets were then sintered to 1250 °C for 12 h. The resulting pellets were approximately 15 mm in diameter and were ground to thickness to 1 mm, and their density was determined to be 93%. Pt films of geometric projected surface area of 1 cm^2 were then painted on each side of the pellets using a Metalor M603B, Pt resinate and sintered to 850 °C for 30 min. The pellets and catalyst films were examined by scanning electron microscopy (SEM) to verify the adhesion of the Pt film on the LSCF support. Pellets A–F were prepared in this way. The weight of the painted Pt film was approximately 10 mg. The BET surface area of the Pt films was estimated to be around 0.4 ± 0.3 m^2. This area was estimated by subtracting the BET area of ten bare LSCF pellets from the BET surface area of ten pellets with Pt films painted on both sides (20 films in total); nevertheless, the uncertainty in the value is high because of the low surface area.

In addition, surface oxygen titration was performed on Pellet D at different temperatures in order to determine the number of Pt active sites on the catalyst film deposited on either side of the membrane. The surface oxygen titration technique consisted of an oxygen adsorption step for $t_{O2} = 10$ min, followed by helium desorption at varied times ($t_{He} = 1.5$–20 min) and reaction with ethylene. By measuring the produced CO_2 during the reaction, the remaining adsorbed oxygen on the Pt surface can be calculated. Plotting the amount of produced CO_2 versus t_{He} and extrapolating to zero (assuming a first-order oxygen desorption process [20]) allows the estimation of the amount of adsorbed oxygen and the number of Pt active sites of the catalyst film (we assume that there is a one-to-one ratio of oxygen to Pt).

In order to prepare the dispersed catalyst system, a Pt catalyst supported on LSCF powder was initially prepared by impregnation by mixing 10 g of LSCF powder and 25 ml of a Pt solution (Sigma ICP standard 987 μg ml^{-1} Pt) and diluting 100 ml with deionised water. The solution was stirred and evaporated using a magnetic stirrer hotplate. The resulting Pt–LSCF slurry was dried to 80 °C to ensure removal of the excess solution and then was sintered to 450 °C for 2 h to obtain adhesion of the Pt onto the LSCF. The resulting Pt–LSCF powder (0.25% weight of Pt) was then mixed with a small amount of ethylene glycol (Sigma) to form a thick paste which was painted on both sides of an LSCF pellet and then sintered to 850 °C to form the dispersed catalyst system (Pellet G). The weight of the painted Pt–LSCF film was approximately 10 mg. The BET surface area of the LSCF powder was approximately 10 m^2 g^{-1}, while the BET surface area of the Pt–LSCF powder was approximately 14 m^2 g^{-1}. However, it would be unreasonable to conclude that the Pt deposited on the LSCF powder has an area of 4 m^2 g^{-1} as it is highly likely that the Pt deposition method could cause structural changes in the support.

Fig. 3 shows SEMs of the Pt film (Fig. 3a) and the dispersed Pt catalyst (Fig. 3b). The pellets used for the SEMs were prepared

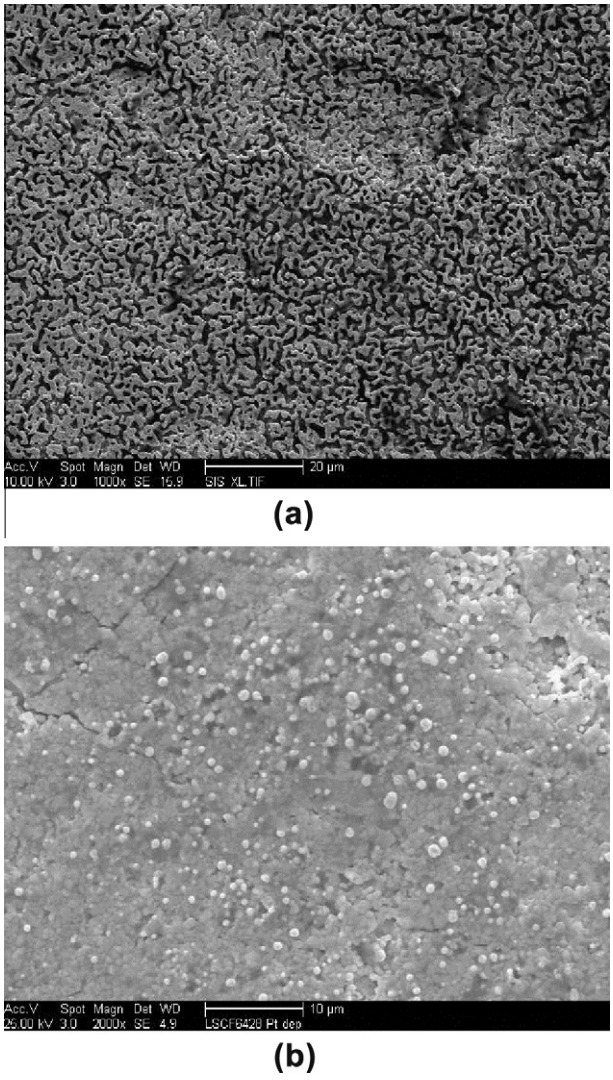

Fig. 3. (a) Typical SEM of a fresh Pt film supported on an LSCF pellet (corresponds to Pellets A–F). (b) SEM of dispersed Pt supported on an LSCF pellets (corresponds to Pellet G).

using the same method and at the same time as the pellets used in the kinetic experiments (Pellets A–F for the film and Pellet G for the dispersed catalyst) but were not used in any kinetic experiments. As can be seen from Fig. 3a, the Pt film shows good porosity in the range of 1–10 μm. The maximum particle size of the dispersed catalyst is less than 1 μm as shown in Fig. 3b, a rather large maximum particle size for a dispersed catalyst. This, with the spherical appearance of the dispersed Pt catalyst particles, may be due to the high sintering temperature (850 °C) and a rather weak interaction between the LSCF and the Pt. It is expected that the geometrical differences between the Pf film and the dispersed catalyst may influence the behaviour of the two systems in terms of the exhibited catalyst modification.

2.2. Kinetic experiments

The catalyst pellets prepared as described previously were mounted in the membrane reactor by using high-temperature glass ceramic sealant. An independent inlet and outlet to either chamber of the reactor allowed control of the gas composition on both reactor chambers. The two chambers could be used as either the reaction chamber (where the reaction takes place) or the sweep chamber where an appropriate sweep gas is used in order to create the chemical potential difference across the membrane that drives the promoter supply. If not otherwise stated, the inner chamber was used as the reaction side and the outer chamber as the sweep side. For the description of the experimental procedure and the discussion of the results, we shall refer to the two chambers as the reaction and sweep side according to their function during the course of the experimental work discussed here.

A set of six gas mass flow controllers (MFC) was used to control the gas composition and flow rate to the two reactor chambers. MFCs 1 and 2 were used for He, 3 for 20% O_2 in He and 4 for 20% O_2 in N_2, 5 and 6 for 10% C_2H_4 in He (all the gases used were research grade supplied by BOC). MFC 6 was also used for the supply of 5%H_2 in He in the sweep side of the reactor. Three modes of operation were used: (1) symmetrical operation where the same reaction mixture and flow rates were fed to both reactor chambers, (2) oxygen operation (referred to as oxygen sweep) where a stream of 20% O_2/He was used in the sweep side in order to create the driving force for oxygen migration towards the reaction side catalyst and (3) hydrogen operation (referred to as hydrogen sweep) where a stream of 5% H_2/He was used to create a driving force for oxygen migration away from the reaction side catalyst. It is expected that under symmetrical operation, there is no driving force for oxygen migration across the membrane and both catalysts should exhibit similar catalytic activity (some variation in the catalytic activity is expected given the catalyst preparation method). The second and third modes of operation were used in order to control the oxygen chemical potential difference across the membrane. A schematic of the membrane reactor and the testing rig can be seen in our previous communication [21].

Typical reaction mixtures used stoichiometric or mildly oxidising ethylene to oxygen ratios. Gas analysis was performed by gas chromatography (Varian GC CP3800) and infra-red spectroscopy (Binos 100 CO/CO_2 analyser and X-Stream 100). The reaction rate is expressed in moles of atomic oxygen reacted and was calculated by measuring the carbon dioxide content at the outlet of the reactor. The area-specific reaction rates refer to the geometric projected surface area of the catalyst film (Pellets A–F) or the Pt–LSCF powder (Pellet G) painted on the LSCF pellets and the turnover-frequencies (Pellet D) to the number of Pt active sites as calculated by oxygen surface titration. In order to be able to determine reaction rates, the reactor was operated under differential conditions (i.e. less than 10% conversion). The experimental rig setup allowed for gas analysis to be performed on both reactor chambers in order to monitor the catalytic activity on both platinum catalysts during the course of the experiment. In some experiments, only the rate of the reaction side was monitored (Pellets A, B, and G). In the experiments conducted with Pellets D, E, and F, the reaction rate on both sides of the membrane was continuously monitored. In the experiments conducted on Pellet C, the rate of the reaction side was continuously monitored while the rate of the sweep side was monitored only at the end of each sweep step, for approximately 20 min under symmetrical operation and prior to the introduction of the next sweep step (the measured rate of the sweep side of Pellet C showed less than 1% variation, so only the average value of the measured rate is shown in the results section). Monitoring the sweep side rate in conjunction with the reaction side rate allows us to draw conclusions as to the cause of any catalytic modification observed during the course of this work on both catalysts.

3. Results

In our early work [18,19], it was shown that the catalytic activity of a metal catalyst film supported onto a MIEC membrane can

be controlled through the influence of an oxygen chemical potential difference across the supporting membrane. Fig. 4 reprinted here from our earlier work [21] for illustrative purposes shows that under the influence of an oxygen chemical potential across the membrane, the catalytic activity of the supported Pt can be enhanced (Pellet A). However, this rate enhancement is not reversible simply by returning to symmetrical operation i.e. zero oxygen chemical potential difference across the membrane (considered as the difference between the oxygen chemical potential on the *tpb* on either side of the membrane) within the same time scale as used for the oxygen sweep. This behaviour was consistent with other experiments (not shown here) performed over longer timescales (up to 10 h). It may be possible that if even longer times are employed for the second symmetrical sweep step, the rate could eventually return to its initial value. Similar results have been seen in the studies of permanent EPOC by the group of Comninellis [22,23]. As discussed in the introduction, the supply of the spillover species in this system can occur via two different routes: (a) via oxygen capture directly from the reaction gas phase (local spillover) and (b) under an oxygen chemical potential difference across the membrane where oxygen migrates across the membrane (remote spillover). Route (a) is possible due to the mixed ionic and electronic conductivity of the support. Route (b) is obviously only possible under an oxygen chemical potential difference across the membrane, while route (a) can take place even under zero oxygen chemical potential difference across the membrane (symmetrical conditions). It has been postulated that the observed activation of the catalyst achieved upon introduction of the oxygen sweep as a result of spillover via route (b) can be sustained through spillover via route (a) upon return to symmetrical operation [19]. In our earlier work, we showed that in order to successfully reverse the observed promotion, the system needs to be operated under the reverse oxygen chemical potential difference (where the driving force allows the migration of oxygen species away from the working catalyst). As mentioned earlier, this is achieved by the use of a hydrogen sweep [18].

Fig. 5 shows a series of different sweeps performed on Pellet B. We can see that during the oxygen sweep, a rate increase of approximately 80% is induced, while during the first hydrogen sweep operation, a rapid rate decrease is observed, leading to a rate that lies 30% lower than the initial reaction rate under symmetrical conditions. During the second cycle, a similar pattern is observed. In this case within the same time scale (as for the first cycle), the rate increase is approximately twofold (with respect to the lowest rate) and 30% with respect to the initial rate under symmetrical conditions. As can be seen from Fig. 5, the induced rate modification occurs over a long period of time (approximately 15 h for the rate increase during the oxygen sweep and 5 h for the rate decrease during the hydrogen sweep). The reason for the long time constants associated with promotional changes may be due to the use of a mixed oxygen ion and electron conductor, LSCF, as a support. Such a support would be expected to be non-stoichiometric under these conditions and will therefore provide an oxygen reservoir and damped response to chemical polarisation.

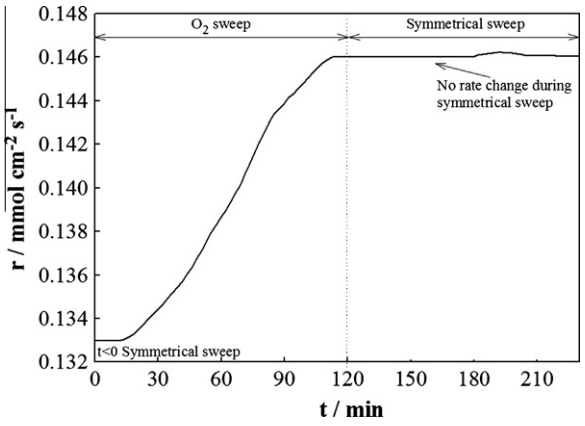

Fig. 4. Reaction rate transient for Pellet A (film catalyst) at 405 °C for a symmetrical-O_2–symmetrical sweep cycle. The experimental conditions were the following: symmetrical sweep (both sides: $p(O_2)$ = 1.5 kPa, $p(C_2H_4)$ = 0.5 kPa, f = 100 ml min^{-1}, oxygen sweep (sweep side): $p(O_2)$ = 19.5 kPa, $p(C_2H_4)$ = 0.5 kPa, f = 100 ml min^{-1}. Reprinted from [21].

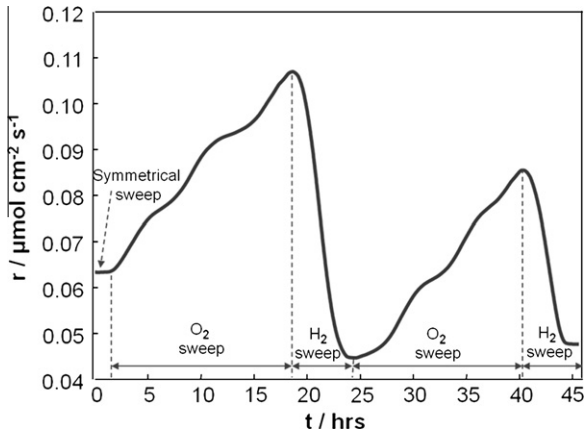

Fig. 5. Reaction rate transient for Pellet B (film catalyst) at 410 °C for two symmetrical-O_2–H_2 sweep cycles. The experimental conditions were the following: symmetrical sweep (both sides: $p(O_2)$ = 2.8 kPa, $p(C_2H_4)$ = 1 kPa, f = 100 ml min^{-1}, oxygen sweep (sweep side): $p(O_2)$ = 20 kPa, f = 100 ml min^{-1}, hydrogen sweep (sweep side): $p(H_2)$ = 5 kPa, f = 100 ml min^{-1}.

In order to further understand the processes occurring in this system and attempt to develop a set of rules that can predict and explain the behaviour of these systems, the effect that oxygen chemical potential differences across the membrane had on the catalysts on either side of the membrane was next investigated. In Fig. 6a, we can see a reaction rate transient (Pellet C) for a series of different modes of operation (symmetrical, oxygen, and hydrogen sweeps) obtained using the inner chamber as the reaction side and outer chamber as the sweep side. Fig. 6b shows a reaction rate transient when the outer chamber was used as the reaction side and inner chamber as the sweep side. In both figures, the continuous line shows the reaction rate of the reaction side, while the discreet data points correspond to the sweep side reaction rate, measured at intervals at the end of each sweep, under symmetrical operation (explained in Section 2). As can be seen from Fig. 6, when each side of the membrane is used as the reaction side (and the gas phase composition remains unchanged throughout the experimental cycle), the measured catalytic rate is influenced by the chemical potential difference across the membrane. In Fig. 6b, this effect is simply demonstrated as stabilisation of the reaction rate and cessation of the oscillations during the first oxygen sweep. Oscillations were occasionally observed in this work (only the example shown in Fig. 6b is presented here). The fact that only one of the two catalyst films of Pellet C shows this oscillatory behaviour could be due to uncharacterised differences in catalyst preparation or the non-identical catalyst history when the rate is determined. Oscillations have been observed in the past in oxidation reactions performed on a Pt catalyst and have been attributed to the periodic formation and dissociation of Pt oxides on the surface of the catalyst ([24,25]). Some rate increase is observed during the second oxygen sweep shown in Fig. 6b. However, the sweep side (where gas phase composition changes occur) shows no rate changes upon return to symmetrical operation (when rates can be measured). It is expected that temporary gas phase composition changes should

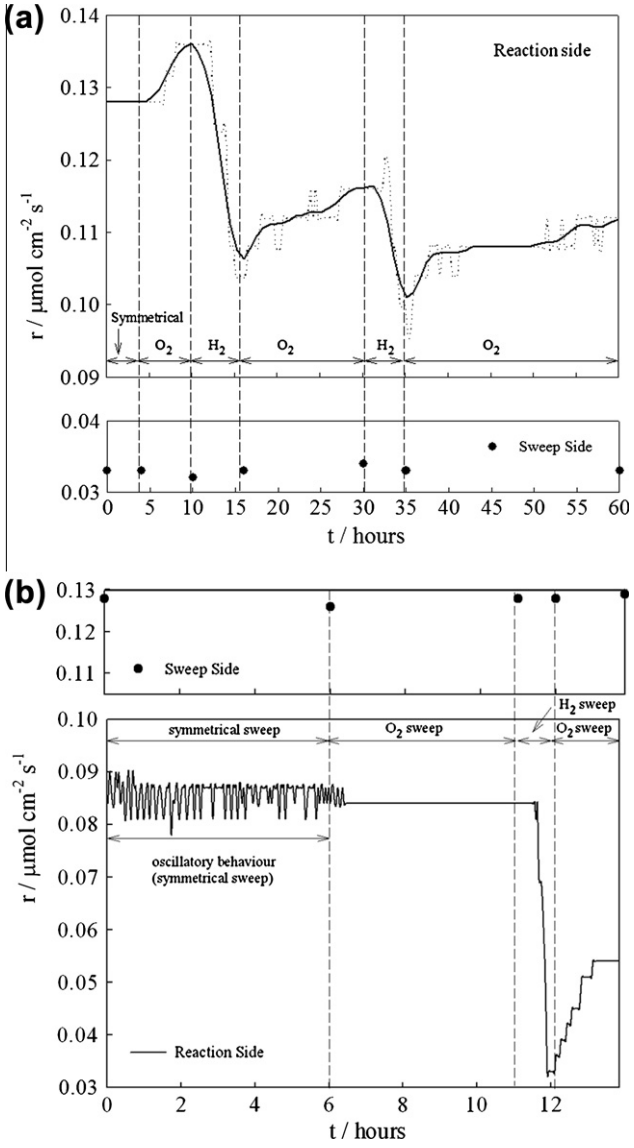

Fig. 6. Reaction rate transient for different experimental cycles at 400 °C for Pellet C (film catalyst), in both figures, the continuous line represents the reaction rate of the reaction side, while the discreet data points correspond to the sweep side reaction rate measured at intervals. In both cases, the experimental conditions were the following: symmetrical sweep (both sides: $p(O_2)$ = 1.3 kPa, $p(C_2H_4)$ = 0.3 kPa, f = 150 ml min^{-1}, oxygen sweep (sweep side): $p(O_2)$ = 20 kPa, f = 150 ml min^{-1}, hydrogen sweep (sweep side): $p(H_2)$ = 5 kPa, f = 150 ml min^{-1}. (a) Inner chamber is used as the reaction side and outer chamber as the sweep side and (b) outer chamber is used as the reaction side and inner chamber as the sweep side.

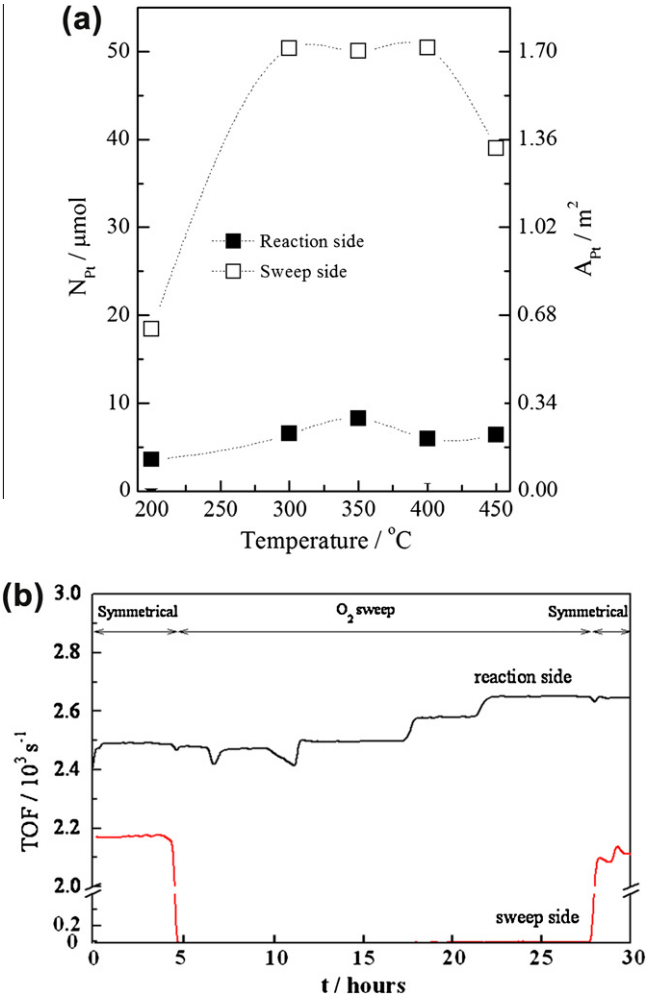

Fig. 7. (a) Number of Pt active sites (N_{Pt}) calculated for surface oxygen titration for Pellet D as a function of temperature. (b) Reaction rate transient at 450 °C showing one experiment symmetrical-oxygen sweep-symmetrical cycle for Pellet D. Both the reaction and the sweep side catalysts are monitored at all times. TOFs are used instead of rate to illustrate the similarity of the two catalyst films despite the different N_{Pt} values calculated. The experimental conditions were the following: symmetrical sweep (both sides: $p(O_2)$ = 1.5 kPa, $p(C_2H_4)$ = 0.5 kPa, f = 120 ml min^{-1}, oxygen sweep (sweep side): $p(O_2)$ = 20 kPa, f = 120 ml min^{-1}.

not permanently affect the catalytic activity of the sweep side. Nevertheless, local spillover also takes place on the sweep side under symmetrical operation and remote spillover should occur when working under an oxygen chemical potential difference (in the opposite way of what occurs in the reaction side), and these processes may be expected to affect the reaction rate of the sweep side. This will be discussed in more detail later.

In Fig. 7, we can see experimental data from a different pellet (Pellet D). Initial experiments conducted on this pellet showed a significant difference in the reaction rates (approximately one order of magnitude difference) on either side of the membrane. This behaviour is in contrast to all of the other pellets which showed similar initial reaction rates on both sides; these rates being similar to that seen on the low reaction rate side of Pellet D. In order to investigate this behaviour further, the number of Pt active sites of the two catalyst films deposited on this pellet was determined via oxygen surface titration at different temperatures and is shown in Fig. 7a. Using a Pt site density of approximately 5×10^{-19} m^2 atom^{-1}, the equivalent Pt surface areas are calculated. We can see that the sweep side catalyst appears to have approximately one order of magnitude more active sites than the reaction side. This significant difference may be due to a poorly controlled method of deposition of the Pt film in this instance. The area of the low surface area Pt film is similar to that measured by BET. In Fig. 7b, we can see reaction turnover frequency (TOF) as a function of time for a symmetrical-oxygen sweep-symmetrical cycle at 450 °C. TOFs have been used in this plot to illustrate the fact that despite the significant difference in the number of Pt sites, the TOFs of the two films are very close. As can be seen in Fig. 7b, introduction of the oxygen sweep results in a modest TOF modification for the reaction side catalyst, this rate modification is not reversed upon return to symmetrical operation. In addition, the activity of the sweep side catalyst remains unaffected upon return to symmetrical operation. This behaviour is consistent with the behaviour of the other pellets as would be expected for a simple difference in surface areas in this case.

In order to assess the role of the sweep gas on the activity of the sweep side catalyst, some experiments were conducted under 'all symmetrical' conditions, i.e. when both sides of the membrane were subjected to the same gas atmosphere at all times so that no oxygen transfer should take place. A series of experiments were performed on Pellets E and F and are shown in Fig. 8a and b. As can be seen from the rate transients in both cases, the reaction rate of both catalyst films returns to the initial rate upon re-introduction of the reaction mixture after the oxygen and hydrogen sweep. The experimental results presented in Fig. 8 aim to illustrate that when the reactor is operated under all symmetrical conditions (reactive or non-reactive), no catalyst modification is observed for either catalyst (obviously under non-reactive conditions, no rates can be measured and any catalyst modification would only be observed upon re-introduction of a reactive gas mixture). These results complement the experiments conducted with an oxygen chemical potential difference across the membrane and taken together demonstrate that a catalyst can be modified only when subjected to both a chemical potential difference across the membrane and when it is in the presence of a reactive gas mixture. In addition, this experiment clearly demonstrates that under non-reactive conditions, the sweep gases (i.e. O_2 and H_2) have no effect on the activity of the catalyst to which they are exposed. Moreover, rate changes observed as a direct result of changes in the gas phase occur very rapidly and cannot be related in any way to changes observed as a result of the promoter supply (as shown in Figs. 4–6) that occur over significantly longer timescales.

One might expect the relative areas of support, catalyst and length of *tpb* in any system to affect the promotional mechanism.

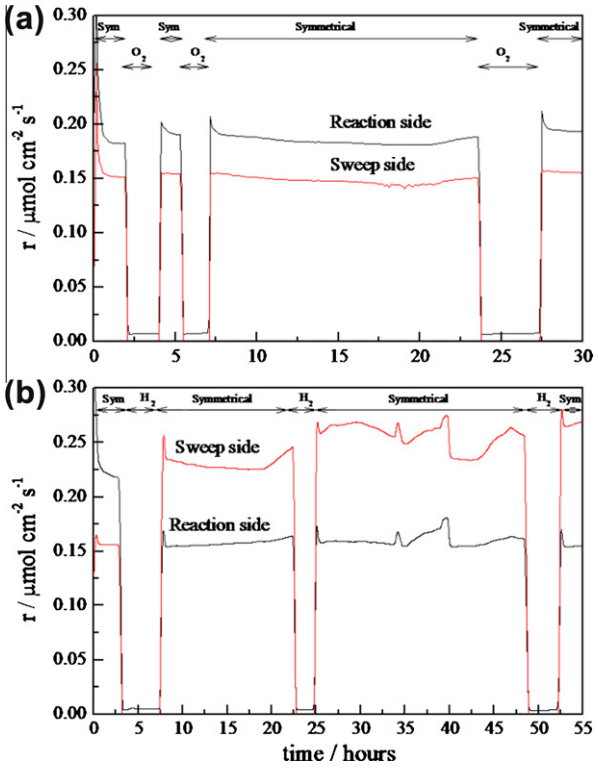

Fig. 8. Reaction rate transients under symmetrical operation only. (a) Pellet E (film catalyst) a series of symmetrical reaction and symmetrical O_2 sweeps are shown. The experimental conditions were the following: symmetrical sweep (both sides: $p(O_2) = 1.5$ kPa, $p(C_2H_4) = 0.5$ kPa, $f = 100$ ml min^{-1}, oxygen sweep (both sides): $p(O_2) = 20$ kPa, $f = 100$ ml min^{-1}. (b) Pellet F (film catalyst) a series of symmetrical reaction and symmetrical H_2 sweep are shown. Symmetrical sweep (both sides: $p(O_2) = 1.5$ kPa, $p(C_2H_4) = 0.5$ kPa, $f = 100$ ml min^{-1}, hydrogen sweep (both sides): $p(H_2) = 5$ kPa, $f = 100$ ml min^{-1}.

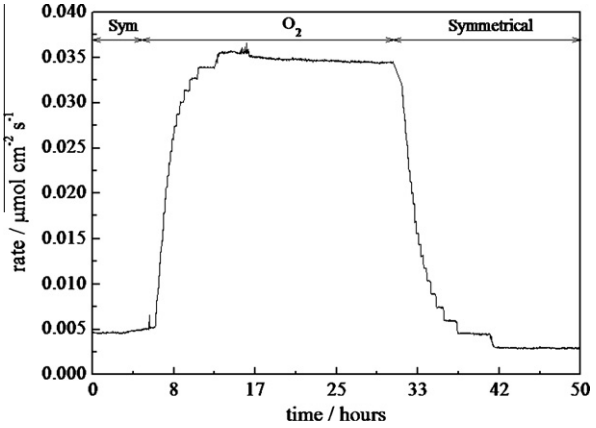

Fig. 9. Reaction rate transient for Pellet G (dispersed catalyst) at 440 °C for a symmetrical-O_2–symmetrical sweep cycle. The experimental conditions were the following: symmetrical sweep (both sides: $p(O_2) = 1.5$ kPa, $p(C_2H_4) = 0.45$ kPa, $f = 115$ ml min^{-1}, oxygen sweep (sweep side): $p(O_2) = 20$ kPa, $f = 115$ ml min^{-1}.

Therefore, it should be possible to fabricate a system of very different geometric arrangement of catalyst on the support that exhibits different behaviour. To test this idea, a sample was fabricated in which the Pt catalyst was not in the form of a continuous film but instead dispersed on the supporting membrane (as described in Section 2). When using a catalyst supported on an MIEC conductor, it is possible to use a non-continuous catalyst as the supporting membrane allows the flux of both oxygen ions and electrons and can therefore provide electrical continuity for the spillover to occur. This is a very important concept as it opens the way for the use for highly dispersed, high surface area catalysts to be used in electrochemical promotion. To the best of our knowledge, the results discussed here are the first obtained using a dispersed Pt catalyst supported on a non-metallic phase for EPOC experiments (i.e. using a two-phase catalyst-support system).[2] Experiments performed using the dispersed Pt–LSCF catalyst supported on an LSCF membrane (Pellet G) at 440 °C showed some very interesting results (initial experiments at 400 °C showed no measurable catalytic rate). As can be seen in Fig. 9 upon introduction of the oxygen sweep, the rate increases significantly from 0.005 μmol cm^{-2} s^{-1} to 0.035 μmol cm^{-2} s^{-1}. This sevenfold increase is also reversible as with return to symmetrical conditions, the reaction rate drops back to the initial value within the same timescale. The duration of the experiment (50 h) is comparable to the duration of experiments performed on the continuous film catalysts, as is the timescale for the observed modification (approximately 10 h for the rate increase under the influence of the oxygen sweep and 10 h for the reversal of the modification). It should to be noted that no hydrogen sweep was used in this experiment for the reversal of the rate modification.

4. Discussion

The results presented in this manuscript indicate that there appears to be a complex interplay between local and remote spillover processes that affects the modification of the Pt catalyst supported on a mixed ionic and electronic conducting membrane. In the case of the continuous Pt film catalyst, the results (shown in Figs. 4–8) allow us to formulate a set of empirical rules that can help us explain and predict the behaviour of the system. In order for

[2] In the past, some experiments on electrochemical promotion have been conducted in what can be viewed as dispersed catalysts that had been nonetheless supported on a nominally inert continuous electronic conducting film, such as gold (e.g. [26,27]) resulting in a three-phase system.

modification of catalytic activity to be observed, we need to have (1) an oxygen chemical potential difference across the membrane (considered, as explained earlier, as the difference between the oxygen chemical potential at the *tpb* on either membrane surface) and (2) the catalyst under investigation should be operated under reaction conditions (i.e. if an oxygen chemical potential difference is imposed by the use of a non-reactive sweep gas then on return to the original reaction conditions, the catalyst exposed to the sweep gas exhibits the original rate). Only when both conditions (1) and (2) are met can the activity of the catalyst be modified. This means that when the system is operated under zero oxygen chemical potential difference, modification 'rate freezing' can be observed (i.e. the rate cannot return to its initial or previous state simply be returning to symmetrical operation). This is illustrated in Fig. 4 where it can be seen that upon return to symmetrical conditions, the observed promotion cannot be reversed. In addition, no activity modification can occur on a catalyst that is not under reaction conditions, even in the presence of an oxygen chemical potential difference across the membrane. This is shown in Fig. 6 where on return to symmetrical operation the rate measured on the sweep side is not modified by the oxygen or hydrogen sweeps. This set of rules agrees with the observed experimental results in all the cases that have been explored so far and should help to predict the behaviour of the system under different experimental conditions.

In order to better understand the mechanistic origins of these rules, we should consider the effect that an oxygen chemical potential difference across the membrane can have on both the local and the remote spillover processes on either side of the membrane. Under the influence of an oxygen chemical potential difference across the membrane, the reaction side of the catalyst becomes the receiver or the donor (depending on the sign of the oxygen chemical potential difference) of promoting oxygen species via the remote spillover process. This is in addition to any local spillover already occurring due to the combination of oxygen present in the gas phase and reaction on the catalyst surface. However, the imposed oxygen chemical potential difference across the membrane may not only affect remote spillover but also the local spillover in a way that leads to a complex response from the system and not simply an additive effect (of the supply of extra spillover oxygen), e.g. if multiple steady states are available to the catalyst. In order to identify some of the possible interactions between the remote and local spillover processes, we need to carefully consider all the driving forces for spillover that exist in this catalyst system under different modes of operation. These are illustrated in Fig. 10. In this figure, driving forces are depicted by arrows. Thick arrows represent the local spillover driving forces and thin arrows the remote spillover driving forces.

Under symmetrical operation (Fig. 10a), there is no oxygen chemical potential difference across the membrane. There exists, however, an oxygen chemical potential difference between the support and the *tpb*. This creates a driving force for local spillover. If we now introduce oxygen to the sweep side of the membrane (Fig. 10b), we impose an oxygen chemical potential difference across the membrane. On the sweep side, there is now no driving force for local spillover due to the absence of reaction; there are of course driving forces for oxygen migration to the *tpb*. On the reaction side, local spillover is still possible. The imposed oxygen chemical potential difference across the membrane results in remote spillover (oxygen consumption at the sweep side *tpb* and oxygen generation at the reaction side *tpb*). Remote spillover will result in a higher spillover rate onto the reaction side catalyst surface. This may allow the catalyst to adopt a new high-rate, high-spillover, steady state. On the sweep side, one might expect the remote spillover to change the catalyst state and that this would be reflected in a modified rate on return to symmetrical conditions. In fact, based on the behaviour of the rate on the reaction side (a rate increase when supplying oxygen to the catalyst and a rate decrease when removing oxygen from the catalyst, previously defined as electrophobic behaviour in EPOC [28]), we may expect the rate on the sweep side to be affected by the imposition of the chemical potential difference across the membrane in the opposite way of the reaction side catalyst. One possible explanation for the lack of this behaviour may be that the surface kinetics are such that the sweep side catalyst state is not significantly modified (perhaps as a result of the ready availability of gas phase oxygen for adsorption on the catalyst versus spillover oxygen) or that an alternative steady state is not reached under the conditions explored in this work. It may be possible that by employing different reaction and/or sweep conditions, we could succeed in inducing a rate modification on the sweep side catalyst as well, as this catalyst could also adopt a new steady state as a result of the spillover of promoting species.

Let us now consider what happens when we return to symmetrical operation (Fig. 10c). On the sweep side, local spillover is reinstated. There is also now a much reduced driving force for remote spillover (dashed arrow in Fig. 10c) as, although the gas feeds are 'symmetrical', the difference in catalyst states introduces an asymmetry. This may be expected to lead to a reduced remote spillover rate to the reaction side. Therefore, if the reaction side catalyst is to maintain its high-rate, high-spillover steady state, it must consume oxygen through a higher rate local spillover process. If this were not possible, then a high-rate steady state would not be maintained and the catalyst would return to its original state and exhibits its original reaction rate. This higher rate local spillover process is facilitated by the mixed conducting support.

Finally, we shall examine the case of the hydrogen sweep shown in Fig. 10d. During the hydrogen sweep, local spillover on the reaction side remains possible. Oxygen promoter species from the reaction side catalyst will be depleted via remote spillover lowering the reaction rate. The lower activity of the catalyst may bring it back to a low-rate, low-spillover state that is maintained on return to symmetrical operation. As in the case of the oxygen sweep, the sweep side catalyst is also subjected to remote spillover during the hydrogen sweep, and we may expect to see a rate modification upon return to symmetrical operation. However, this is not the case and an alternative steady state is not seen.

It is interesting that the dispersed Pt catalyst (Fig. 9) behaves quite differently to the continuous Pt film in terms of the promotion reversal, i.e. the reaction rate returns to the initial value upon return to symmetrical operation, instead of remaining at the modified value as was the case of the continuous film. This different behaviour may be attributed to the different geometric arrangement of the catalyst and support interface of the two systems. Recall that the relative surface areas of the two catalysts are different by at least one order of magnitude and that will affect the relative *tpb* lengths of the two catalyst systems as well. It is postulated that the different Pt geometry of the two systems may affect the relative rates of the local and remote spillover processes. It appears that in this case, the role of remote spillover becomes significantly more important than that of local spillover and this may be the reason why the behaviour of the system resembles that of a classic EPOC experiment (where the catalyst is supported on a purely ionic conductor, a solid electrolyte, and therefore significant local spillover cannot take place due to the lack of electronic conductivity of the support), i.e., initiation of the remote spillover process (by an oxygen sweep) modifies the reaction rate and cessation of the remote spillover leads to reversal of the rate modification. As in EPOC, the species already present on the catalyst surface due to remote spillover is eventually consumed via the reaction and the rate modification will be reversed.

The systems investigated here can be seen as intermediates between a 'real' catalyst and the catalysts used for electrochemical

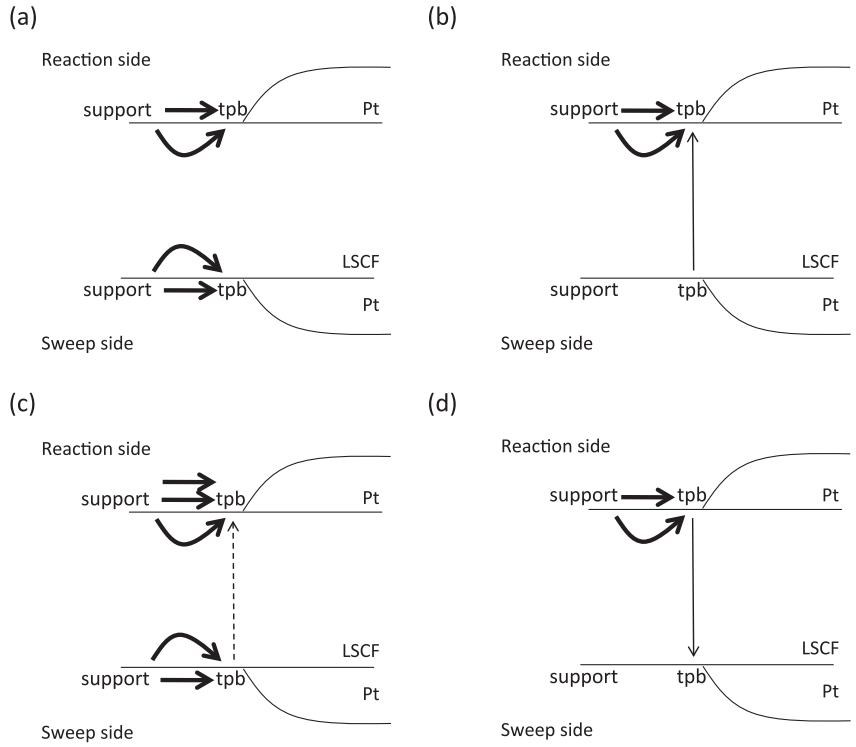

Fig. 10. Schematic representation of spillover processes on the catalyst system: (a) symmetrical operation, (b) oxygen sweep, (c) return to symmetrical operation after oxygen sweep and (d) hydrogen sweep.

promotion experiments. In a real catalyst (where the active phase is dispersed on a mixed conducting support), only local spillover can take place (due to activity and chemical potential differences between the catalyst and the support), and it is not possible to control spillover and modify the catalytic activity *in situ*. At the other extreme, the systems were studied in EPOC (with catalysts supported on ionic conductors) where local spillover does not take place but one can have full control of the induced catalytic activity modification via the control of remote spillover. In the systems studied in this work, both local and remote spillover processes appear to co-exist. As in the case of a real catalyst, the existence of local spillover reduces the control possible over the rate modification. However, through changing the relative importance of remote and local spillover by altering the catalyst geometry, it is possible to move towards a system that is more closely related to an EPOC catalyst and therefore regain more external control.

5. Conclusions

The effect of spillover processes on the activity of a catalyst system consisting of a mixed oxygen ion and electronic conducting support $La_{0.6}Sr_{0.4}Co_{0.2}Fe_{0.8}O_{3-\delta}$ and a metal catalyst (Pt) were investigated. A model single-pellet was used employing Pt catalysts deposited on both sides of a dense LSCF disc pellet. Driving forces for promoter migration were controlled through the manipulation of the oxygen chemical potential difference across the membrane. Catalyst rate modification was observed. In the case of a continuous, low dispersion, catalyst film a rate promotion was seen when oxygen was supplied to the reaction side as a result of the presence of an oxygen sweep gas. However, when the oxygen sweep gas was removed, the rate on the reaction side did not return to its original value, indicating that the catalyst had taken on a new higher reactivity state. This state would require a higher promoter supply, and this appears to come from oxygen capture by the support surface on the reaction side. It was postulated that the relative rates of spillover and reaction and the relative areas of support and catalyst would influence such behaviour. This was confirmed in a separate experiment in which a highly dispersed Pt catalyst (non-continuous) was used. The behaviour with this catalyst was reminiscent of classical electrochemical promotion possibly because of the different competition between alternative forms of spillover.

Acknowledgements

The authors would like to acknowledge the financial support of the Engineering and Physical Sciences Research Council (Grant Numbers EP/E033687/1 and EP/G025649/1).

References

[1] B. Delmon, Solid State Ionics 101–103 (Part 2) (1997) 655.
[2] B. Delmon, Catalysis Today 117 (1–3) (2006) 69.
[3] J. Pritchard, Nature 343 (1990) 592.
[4] C.G. Vayenas, S. Brosda, C. Pliangos, Journal of Catalysis 216 (1–2) (2003) 487.
[5] I.V. Yentekakis, M. Konsolakis, R.M. Lambert, A. Palermo, M. Tikhov, Solid State Ionics 136–137 (2000) 783.
[6] G.L. Haller, Journal of Catalysis 216 (1–2) (2003) 12.
[7] D.E. Resasco, G.L. Haller, Applied Catalysis 8 (1) (1983) 99.
[8] S. Brosda, C.G. Vayenas, J. Wei, Applied Catalysis B: Environmental 68 (3–4) (2006) 109.
[9] A. Katsaounis, Z. Nikopoulou, X.E. Verykios, C.G. Vayenas, Journal of Catalysis 222 (1) (2004) 192.
[10] C.G. Vayenas, D. Archonta, D. Tsiplakides, Journal of Electroanalytical Chemistry 554–555 (2003) 301.
[11] A. Thursfield, I.S. Metcalfe, Journal of Membrane Science 288 (1–2) (2007) 175.
[12] S.J. Xu, W.J. Thomson, Chemical Engineering Science 54 (17) (1999) 3839.
[13] C.G. Vayenas, S. Bebelis, Catalysis Today 51 (3–4) (1999) 581.
[14] C.G. Vayenas, S. Brosda, C. Pliangos, Journal of Catalysis 203 (2) (2001) 329.
[15] I.S. Metcalfe, S. Sundaresan, AIChE Journal 34 (2) (1988) 195.
[16] E. Papaioannou, S. Souentie, F. Sapountzi, A. Hammad, D. Labou, S. Brosda, C. Vayenas, Journal of Applied Electrochemistry 40 (10) (2010) 1859.
[17] E.A. Baranova, G. Foti, C. Comninellis, Electrochemistry Communications 6 (2) (2004) 170.
[18] D. Poulidi, C. Anderson, I.S. Metcalfe, Solid State Ionics 179 (27–32) (2008) 1347.

[19] D. Poulidi, A. Thursfield, I. Metcalfe, Topics in Catalysis 44 (3) (2007) 435.
[20] C.G. Vayenas, S. Bebelis, C. Pliangos, S. Brosda, D. Tsiplakides, Electrochemical Activation of Catalysis Promotion, Electrochemical Promotion, and Metal–Support Interactions, Kluwer/Plenum, New York, 2002.
[21] D. Poulidi, I. Metcalfe, Journal of Applied Electrochemistry 38 (8) (2008) 1121.
[22] C. Falgairette, A. Jaccoud, G. Folti, C. Comninellis, Journal of Applied Electrochemistry 38 (8) (2008) 1075.
[23] S. Souentie, C. Xia, C. Falgairette, Y.D. Li, C. Comninellis, Electrochemistry Communications 12 (2) (2010) 323.
[24] P. Beatrice, C. Pliangos, W.L. Worrell, C.G. Vayenas, Solid State Ionics 136–137 (2000) 833.
[25] I.V. Yentekakis, C.G. Vayenas, Journal of Catalysis 111 (1) (1988) 170.
[26] S. Balomenou, G. Pitselis, D. Polydoros, A. Giannikos, A. Vradis, A. Frenzel, C. Pliangos, H. Pütter, C.G. Vayenas, Solid State Ionics 136–137 (2000) 857.
[27] C. Xia, M. Hugentobler, Y. Li, G. Foti, C. Comninellis, W. Harbich, Electrochemistry Communications 13 (1) (2011) 99.
[28] C. Vayenas, S. Brosda, Solid State Ionics 154–155 (2002) 243.